

Adaptive Sine-Modulated/Cosine-Modulated Filter Bank Equalizer for Transmultiplexers

Juuso Alhava* and Markku Renfors*

Abstract — Cosine-modulated filter banks provide an efficient realization for filter bank-based transmultiplexers. This paper describes an equalization method for these systems. At the receiver we have two parallel analysis filter banks (cosine- and sine-modulated FBs) whose subchannel outputs are combined optimally. This increases the computational burden on the filter bank side, but very simple subchannel equalizer structure is a clear advantage. For adaptive implementation, the number of required general multipliers is reduced, and it is possible to develop LMS-based equalization algorithms with fast convergence. Therefore, the equalizer structure is called as Adaptive SMFB/CMFB Equalizer for Transmultiplexers (ASCET).

1 Introduction

Recently, there has been a growing interest to use existing subscriber lines for providing broadband access to customers. Multicarrier modulation can reach high efficiency in these frequency selective channels. In multicarrier systems, a raw bit stream is transmitted with numerous low bit rate subcarriers. The number of subcarriers should be large enough to make the subchannel bandwidth below the coherence bandwidth of the channel. Then the channel is frequency flat within the subchannel bandwidth [1]. However, it should be remembered that increasing the number of carriers (or subchannels) is not always possible due to latency, implementation complexity, and channel coherence time (multicarrier symbol length is depending on the number of carriers).

OFDM is the prominent multicarrier system of today and it is applied, e.g., in digital audio/video broadcasting. Baseband version of OFDM is called as discrete multitone (DMT) modulation. The channel equalization is done similarly in both systems. A cyclic prefix is appended to transmitted symbols to mitigate intersymbol interference (ISI) and intercarrier interference (ICI). Then a single complex multiplier per subchannel is sufficient to correct phase and amplitude [2]. The cyclic prefix approach somewhat reduces the transmission rate. In OFDM/DMT, another drawback is the use of discrete Fourier transform-basis, which does not provide high selectivity. When the channel has very strong narrowband interference, OFDM/DMT

suffers more than filter bank-based transmultiplexers (TMUX), which can be designed to have good selectivity [3].

Here we consider TMUX equalization for critically subsampled filter banks (FB) based on cosine-modulated implementation structure (CMFB) [5]. The cyclic prefix equalization approach is out of question, because transmitted symbols are overlapping. One possibility is to use multiple input-multiple output (MIMO) combiners to remove interference [3][4], but clearly they do not share the elegance and simplicity of the OFDM equalization.

This paper contributes to the equalization issue with a practical idea that can be applied with CMFBs. In the baseband channel case, we add a sine-modulated FB (SMFB) to co-operate with the CMFB in signal equalization. Due to simplification of the adaptive part, we use the name Adaptive SMFB/CMFB Equalizer for Transmultiplexers (ASCET) for this system. We also demonstrate how it is possible to construct a similar scheme for passband channels, and still enjoy the advantages of fewer adaptive coefficients.

Filter bank-related notations are used as in [6]: M is the number of subchannels and overlapping factor K controls the subchannel filter length.

2 Proposed Equalizer Structure

2.1 Zero-Order ASCET

We introduce the ASCET structure in two parts: zero-order and higher order ASCETs. The zero-order equalizer structure provides some insight to the equalization idea, how the receiver in Figure 1 can recover the transmitted symbol sequence.

The analysis and synthesis filters for CMFBs are formed from a single prototype filter $h_p(n)$ in the following way:

$$h_k^c(n) = 2 h_p(n) \cos \left((2k+1) \frac{\pi}{2M} \left(n - \frac{N}{2} \right) + (-1)^k \frac{\pi}{4} \right) \quad (1)$$

and

$$f_k^c(n) = 2 h_p(n) \cos \left((2k+1) \frac{\pi}{2M} \left(n - \frac{N}{2} \right) - (-1)^k \frac{\pi}{4} \right), \quad (2)$$

where $n = 0, 1, \dots, N-1$ ($N = 2KM-1$). CMFBs have efficient implementation structures, such as fast ELT [6]. Some implementation aspects related to this application were covered in [7].

*Telecommunication Laboratory, Tampere University of Technology, P.O. Box 553, FIN-33101, Tampere, FINLAND. E-mail: Juuso.Alhava@tut.fi

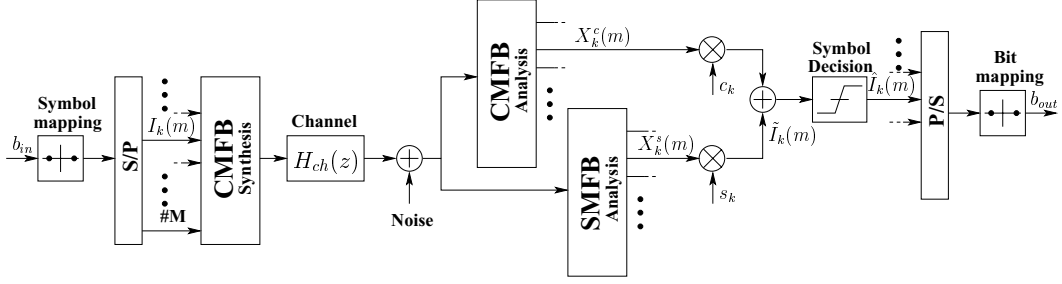


Figure 1: Zero-order ASCET structure.

When the receiver is compared with the MIMO-equalizer, we have a new element: sine-modulated FB. The subchannel filters for this bank are formed by changing the phase of the modulating frequency in equation (1),

$$h_k^s(n) = 2 h_p(n) \sin\left((2k+1)\frac{\pi}{2M}\left(n - \frac{N}{2}\right) + (-1)^k \frac{\pi}{4}\right). \quad (3)$$

The superscripts s and c in the notations refer to sine and cosine modulated FBs, respectively. Subchannel signals $X_k^c(m)$ and $X_k^s(m)$ are combined after multiplying them with two equalizer coefficients c_k and s_k . Thus only two parameters are optimized per subchannel, and this optimization is independent from all other subchannels.

The next question is: "Why this equalization scheme works?" The parameters c_k and s_k can provide us the answer, when we observe that the equalizer coefficients are connected with the channel amplitude and phase responses as follows:

$$A_{ch}(\omega_k) = |H_{ch}(e^{j\omega_k})| \approx 1/\sqrt{c_k^2 + s_k^2}$$

$$\phi_{ch}(\omega_k) \approx \pm \tan^{-1}\left(\frac{s_k}{c_k}\right),$$

where $k = 0, 1, \dots, M-1$. The sign of the above phase angle is determined from the signs of c_k and s_k by choosing the correct quadrant. To demonstrate this, we take a simple noiseless channel model $H_{ch}(z) = 1/(1 - .9z^{-1})$ and find the optimal equalizer coefficients (see Section 2.3 how it is done). The phase and amplitude responses of the channel are shown in Figure 2 and the estimates from the equalizer are marked with crosses.

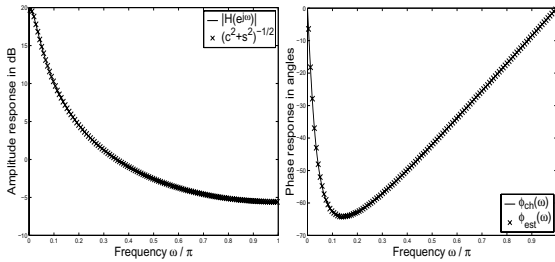


Figure 2: Channel amplitude response (left) and phase response (right) as seen from c_k and s_k

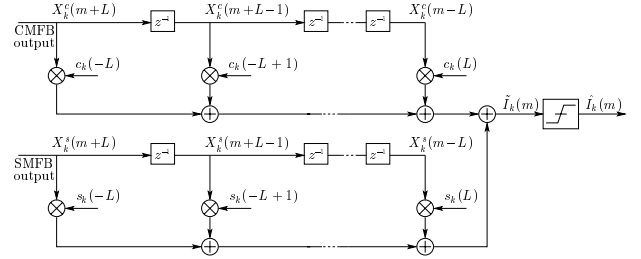


Figure 3: $2L$ -order ASCET receiver structure.

These remarks allow us to write the coefficients in a more convenient form

$$c_k \approx \frac{1}{A_{ch}(\omega_k)} \cos(\phi_{ch}(\omega_k)) \quad s_k \approx \frac{1}{A_{ch}(\omega_k)} \sin(\phi_{ch}(\omega_k))$$

Now we can write the k th subchannel filter $h_k^{cs}(n)$ using (1) and (3)

$$h_k^{cs}(n) = \frac{2}{A_{ch}} \cos(\phi_{ch}) h_p(n) \cos\left((2k+1)\frac{\pi}{2M}\left(n - \frac{N}{2}\right) + (-1)^k \frac{\pi}{4}\right) + \frac{2}{A_{ch}} \sin(\phi_{ch}) h_p(n) \sin\left((2k+1)\frac{\pi}{2M}\left(n - \frac{N}{2}\right) + (-1)^k \frac{\pi}{4}\right) = \frac{2}{A_{ch}} h_p(n) \cos\left((2k+1)\frac{\pi}{2M}\left(n - \frac{N}{2}\right) + (-1)^k \frac{\pi}{4} - \phi_{ch}\right) \quad (4)$$

This means that the structure gives us the control over phase and amplitude of the modulated receiver filters.

2.2 Higher Order ASCETs

The equalizer structure in Figure 1 is sufficient for channels, where the channel frequency response does not have fast variation within subchannel bandwidth. But if this is not satisfied, the equalizer performance is limited by self-interference. Especially, this is observed when the background noise power is very low, and ICI/ISI will give a noise floor for poorly equalized subchannels. Increasing the number of the subchannels brings improvement, but as discussed before, this is not always possible.

Fortunately, the system performance can be made better with modest increase in the computational effort. We add delays and multipliers after both banks, and combine the outputs as shown in Figure 3. The ASCET equalizer order N_A defines

the length of delay line. For convenience we use $L = N_A/2$ in equations and figures (N_A is even). N_A th order subchannel equalizer has therefore $4L$ delay elements and $4L + 2$ adaptable multipliers.

It would be a waste of resources, if we apply the higher order ASCET for low SNR-subchannels. Therefore, it is practical to construct a mixed ASCET equalizer, where higher order equalizers handle subchannels with high SNR, and the two coefficient equalizer is adequate for the rest. For example, in VDSL channel we should be prepared to use more equalization power in the lower frequency range.

2.3 MMSE Solution for ASCET Receiver

Now we derive the optimal coefficients for the N_A th order receiver operating in a stationary channel. The Minimum Mean Squared Error (MMSE) problem is decoupled (equalizer coefficients for subchannel k can be derived independently from all other subchannels), and we write the equalizer coefficients for subchannel k :

$$\underline{\mathbf{c}}_k = [c_k(-L) \quad c_k(-L+1) \quad \dots \quad c_k(L) \quad \dots \quad s_k(-L) \quad s_k(-L+1) \quad \dots \quad s_k(L)]^T. \quad (5)$$

The equalizer input at instant m is

$$\underline{\mathbf{X}}_k(m) = [X_k^c(m+L) \quad X_k^c(m+L-1) \quad \dots \quad X_k^c(m-L) \quad \dots \quad X_k^s(m+L) \quad X_k^s(m+L-1) \quad \dots \quad X_k^s(m-L)]^T. \quad (6)$$

With the aid of (5) and (6) we can write the familiar form for the MSE function

$$\mathcal{E}_{MSE,k} = E \left[|I_k(m) - \underline{\mathbf{c}}_k^T \underline{\mathbf{X}}_k(m)|^2 \right]. \quad (7)$$

The problem is to find such coefficients $\underline{\mathbf{c}}_k$ that minimize equation (7). If we denote the autocorrelation matrix of $\underline{\mathbf{X}}_k(m)$ by

$$\mathbf{R}_k = E[\underline{\mathbf{X}}_k(m)\underline{\mathbf{X}}_k^T(m)], \quad (8)$$

and the cross-correlation vector between $I_k(m)$ and $\underline{\mathbf{X}}_k(m)$ by

$$\underline{\mathbf{p}}_k = E[I_k(m)\underline{\mathbf{X}}_k(m)], \quad (9)$$

we get the the optimal MMSE solution

$$\underline{\mathbf{c}}_{k,o} = \mathbf{R}_k^{-1} \underline{\mathbf{p}}_k. \quad (10)$$

Using equations (8-10) we obtained the coefficients for the curves in Figure 2 ($L = 0$).

3 ASCET for Passband Channels

The ASCET transceiver structure can also be introduced for passband transmission systems. A passband channel can be modeled with an equivalent (complex) lowpass channel [1]. Without further derivation, Figure 4 presents the 0th order ASCET. The rather curious indexing (k and $-(k-1)$,

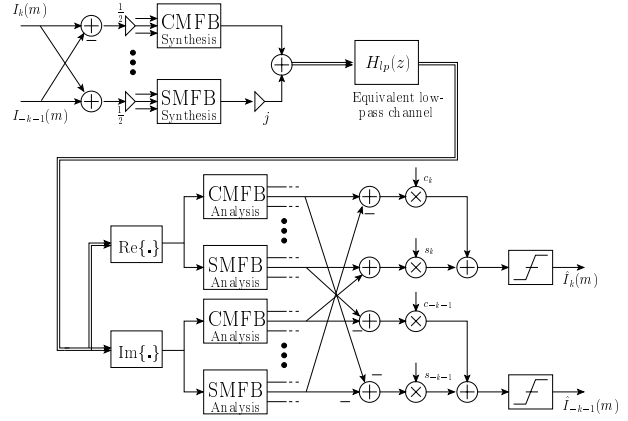


Figure 4: 0th order Complex ASCET

$k = 0, 1, \dots, M-1$) originates from the observation that using MMSE-solution for c_i and s_i , these coefficients relate to the channel frequency response. The little difference compared with the baseband channel comes when $i < 0$. These coefficients correspond to negative frequencies ($H_{lp}(e^{j\omega})$ nonsymmetric), but it should be noted that the indexing (or signs) in Figure 4 applies for odd values of K .

It should be emphasized that the complex ASCET transmits real symbols $I_k(m)$ and $I_{-k-1}(m)$ independently from each other. The largest portion of the transmission power for subchannels with index $k > 0$ is located on the positive side of the spectrum. The receiver is able to recover the signal by combining the outputs of the analysis banks as in Figure 4 and then we can use the results of the Section 2.3 to combine the subchannel signals. A more detailed analysis of this complex ASCET-system is left for future, but some results are shown in the following section.

4 Examples

4.1 Effect of N_A and M to SIR

We use the ASCET-structure to demonstrate how the number of subchannels M and equalizer order N_A impacts on signal to interference ratio (SIR). Again we use simple channel model $H_{ch}(z) = 1/(1 - .9z^{-1})$. Otherwise, the channel is noiseless and thus all interference comes from the imperfection in the equalization. We use the MMSE solution for $\underline{\mathbf{c}}_k$, and measure the SIR at the equalizer output

$$\text{SIR}_k = 10 \log_{10} \frac{\sigma_{I_k}^2}{\sigma_{e_k}^2},$$

where $\sigma_{I_k}^2$ is the variance of the random symbol sequence $I_k(m) = \pm 1$ for subchannel k and $\sigma_{e_k}^2$ is variance of the error sequence $e_k(m) = I_k(m) - \hat{I}_k(m)$.

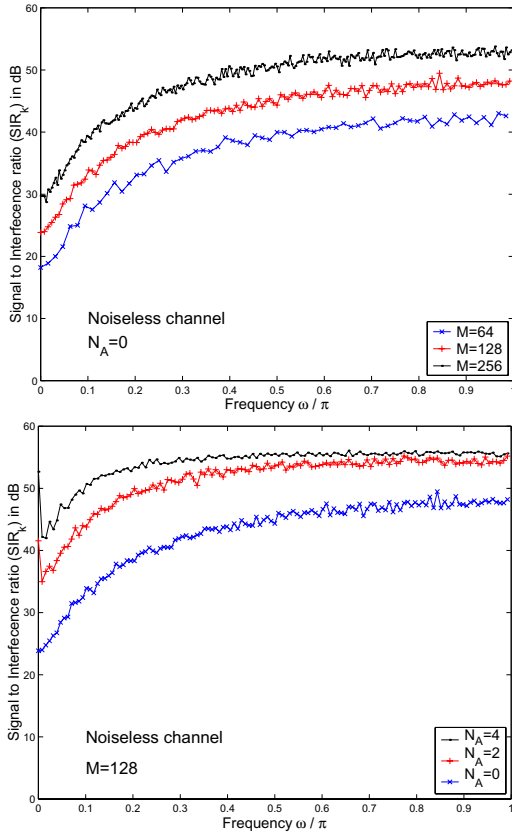


Figure 5: Signal to interference ratio of the ASCET equalizer, when the equalizer order N_A and the number of the subchannels M is varied. The channel is $H_{ch}(z) = 1/(1 - .9z^{-1})$ and noiseless. ($K = 5$)

By looking at the SIR-curves in figure 5 we find that by doubling M we should expect about 6 dB improvement in SIR. In practice, the channel noise limits the highest possible SIR. The other figure shows how higher order equalizers can get rid of the notch in SIR-curves near the zero frequency.

4.2 Complex ASCET and OFDM

We close this article by showing SIR-curves for a complex ASCET with the following parameters: $M = 64$, $K = 5$, $N_A = 0$ or 2 , and $H_{ch}(z) = e^{-j\pi/3} + .5e^{-j\pi/5}z^{-2} + .1e^{-j\pi/7}z^{-7}$. Background AWGN power is 35 dB below received signal power and there is a strong narrowband interference present at the normalized frequency $f_{nb} = 0.26$. A similar curve is shown for 128-channel OFDM with sufficiently long cyclic prefix. Noise levels were chosen to make the difference visible between the three cases. The curves in Figure 6 show how narrowband noise degrades several OFDM-subcarriers, whereas FB-TMUX loses only few subchannels. The other factor in considerations is the length of cyclic prefix, which further reduces the capacity of the OFDM-system.

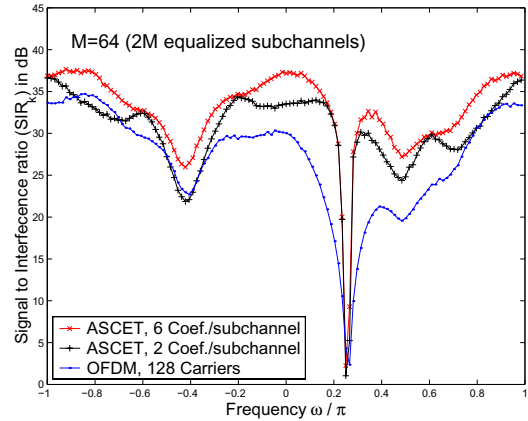


Figure 6: Complex ASCET SIR curves for order 0 and 2. OFDM SIR is shown for reference.

5 Conclusions

This paper demonstrated how CMFB and SMFB can be applied together in FB-based transmultiplexers to reduce the complexity of the adaptive part. The approach is attractive from the implementation point of view, since we have to implement less general multipliers at the receiver.

In future work, we will present fast converging equalization algorithms for the transmission system described in this paper and consider its performance in difficult channel environments: powerline communications, VDSL with narrowband interference, and broadband WLANs.

References

- [1] J. Proakis, *Digital Communications*, McGraw-Hill, 3rd ed., 1995.
- [2] R. van Nee and R. Prasad, *OFDM for Wireless Multimedia Communications*, Artech House, 2000.
- [3] S. Sandberg and M. Tzannes, "Overlapped discrete multitone modulation for high speed copper wire communications," *IEEE Journal on Selected Areas in Communications*, vol. 13, pp. 1571-1585, 1995.
- [4] J. Louveaux, L. Vandendorpe, L. Cuvelier, F. Deryck, and O. van de Wiel, "Linear and decision-feedback MIMO equalization for transmultiplexer-based high bit rate transmission over copper wires," *Broadband Communications, 1998. Accessing, Transmission, Networking*, Zurich, pp. 177-184, 1998.
- [5] P. Vaidyanathan, *Multirate Systems and Filter Banks*, Englewood Cliffs, NJ: Prentice Hall, 1993.
- [6] H. Malvar, "Extended lapped transforms: Properties, applications and fast algorithms," *IEEE Transactions on Signal Processing*, vol. 40, pp. 2703-2714, Nov. 1992.
- [7] A. Viholainen, J. Alhava, and M. Renfors, "Implementation of Parallel Cosine and Sine Modulated Filter Banks for Equalized Transmultiplexer Systems", submitted to *Int. Conf. Acoust., Speech, Signal Processing*, Salt Lake City, Utah, 2001.